Length of Phenolic Strings in Dissolution Inhibition Resists

Yu-Kai Han and Arnost Reiser*

Institute of Imaging Sciences, Polytechnic University, Brooklyn, New York 11201

Received July 13, 1998; Revised Manuscript Received September 14, 1998

ABSTRACT: We have determined the inhibition strength of a group of difunctional naphthalene-1-sulfonic acid esters. In these structures the sulfonic acid groups were placed at increasing distances from each other by using aromatic dihydroxy compounds as spacers. At short distances the inhibition factors of the difunctional compounds are much smaller than the sum of the inhibition factors of the monofunctional sulfonic acid groups, and we interpret this as the result of interference between the phenolic strings emanating from the S=O dipoles of the sulfonic acid moieties. By systematically increasing the distance between the sulfonic acid groups, we were able to determine the critical distance at which their strings no longer influence each other. We believe that in this way we have found the radius of gyration and hence the length of the undisturbed strings.

Introduction

When a hydrogen acceptor, such as a ketone or a sulfone, is introduced into a solution of novolak or another phenolic resin, it forms a hydrogen bond with a nearby OH group and in so doing polarizes it. The oxygen atom of the polarized phenol carries now a larger than usual partial negative charge, which makes it in turn a better hydrogen acceptor. It attracts another hydroxyl that is thereby polarized, etc. In this way a string of hydrogen-bonded OH groups is formed.[1,2]

The strings formed in the coating solution survive into the solid film, and they are the agents of dissolution inhibition. How can they affect the dissolution rate? Recent experiments[3] with deuterated novolak and deuterated developers have shown that the dissolution of novolak films is controlled by the deprotonation of its phenol units.

$$POH + OH^- \rightarrow PO^- + H_2O$$

Deprotonation may be viewed as a two-step process: the first step is the dissociation of phenol into a phenolate ion and a proton

$$POH \rightarrow PO^- + H^+$$

and the second step is the neutralization of the proton by base.

$$H^+ + OH^- \rightarrow H_2O$$

It follows that in a solid environment the rate of deprotonation, and hence the rate of film dissolution, R, depend not only on the local concentration of base, c_B, but also on the concentration of protons, c_{H^+}, in equilibrium with the local, polymer-bound phenols.

$$R = kc_Bc_{H^+} \quad (1)$$

The phenolic protons in the strings are bound more firmly than the protons of free phenols in the bulk of the solution. In terms of eq 1 the inhibitor-induced strings affect dissolution by lowering the (average) proton concentration, c_{H^+}. This implies a connection between string characteristics and inhibition.[4]

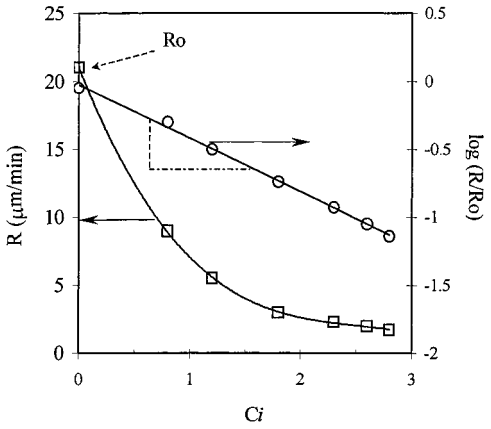

Figure 1. Meyerhofer plot of log R vs c_i and determination of the inhibition factor. R is the dissolution rate (μm/min), and the concentration of inhibitor, c_i, is in mol/L or mol/1000 g of resin.

String Characteristics and the Inhibition Factor

We have shown[4] that phenolic strings are characterized by their length (n) and by the mean dissociation constant or pK_a of their phenols. To test the effect of an additive on the dissolution rate of the resin, we measure the dissolution rate, R, of resin films containing increasing concentrations of the additive. The inhibitor strength of the additive is then characterized by an inhibition factor, f, defined as the negative slope of a plot of log R vs the inhibitor concentration, c_i, in the resist film.[5,6] Figure 1 shows such a plot.

The corresponding plots for the difunctional inhibitors of this study are shown in Figure 2.

$$f = -\frac{\mathrm{d}\log R}{\mathrm{d}c_i} \quad (2)$$

The link between the inhibition factor and the characteristics of phenolic strings is summarized in eq 3, which

10.1021/ma981090j CCC: $15.00
Published on Web 11/20/1998

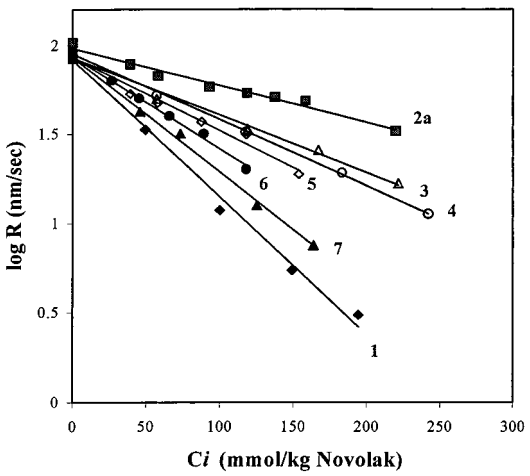

Figure 2. Meyerhofer plots, log R vs c_i, for a series of difunctional sulfonic acid inhibitors.

was derived in ref 4.

$$f = n\,\frac{\log e}{c_{OH}}\left[1 - \frac{c_{H(b)}}{c_{H(a)}}\right] \qquad (3)$$

Here $\log e = 0.4343$, n is the string length, and $c_{H(a)}$ and $c_{H(b)}$ are the proton concentrations in equilibrium with free and with bound phenols. They can be obtained from electrochemical (pH) measurements,

$$c_{H^+} = 10^{-pH}$$

Once the bound and free proton concentrations are known, eq 3 may be used to calculate string length from inhibition factors. In that case the phenol concentration c_{OH} refers to the conditions of the coating solution where the strings are actually formed. For a coating solution containing the standard 25 wt % of resin, $c_{OH} = 2.08$ M. The inhibition factor (in reciprocal moles per liter) of the typical sulfonic acid inhibitor used in this study is $f = 0.77$, and the bracket in eq 2 has a value of 0.369.[4] Using these data, one finds a string length of $n = 10.0$. In the rather different conditions of the electrochemical experiments the string length was found as 14.3.[4]

String length is here defined as the number, n, of OH groups attached by hydrogen bonding to the acceptor moiety of the inhibitor. The space over which the string extends may be characterized by a radius of gyration, R_G, which is defined in the same way as the radius of gyration of a polymer chain. Phenolic strings are shorter than the chains of common polymers, and so the statistical predictions of the theory will not be fulfilled with the same accuracy, but we believe that the same principles apply. The radius of gyration is related to the number of units (n) in the string and to the length of the string segment λ. The segment length in phenolic strings is that of the bond sequence

O----H.....O

0.96 3.03

4.0 Å

The radius of gyration is proportional to the square root of string length n.[7]

$$R_G = \frac{3\alpha\lambda}{6}\sqrt{n} \qquad (4)$$

The factor α was introduced by Flory and Fox[8] to take account of intersegmental interactions. It is unity in poor solvents and larger than one in good solvents, such as ours (cyclohexanone). Setting for the time being $\alpha = 1$, one obtains for the sulfonic acid inhibitor of the preceding section the following radius of gyration (in angstrom units).

$$R_G = \frac{3 \times 4.0}{6}\sqrt{10.0} = 6.3\ \text{Å}$$

In the foregoing, string length had been determined from inhibition factors together with information derived from electrochemical experiments. It would be highly desirable to confirm these results by an independent route. We believe that we have found such an approach in the phenomenon of string interference.

Interference between Strings

It has been variously observed[9,10] that the inhibition strength of polyfunctional inhibitors, namely those that carry more than one acceptor group, is significantly smaller than the sum of the inhibition factors of the individual acceptors. In terms of a model of inhibition based on phenolic strings it is not unreasonable to think that this effect is caused by string interference. Strings that emanate from individual, yet not too distant, acceptor (anchor) groups interfere in the sense that they do not allow each other to grow to their full unhindered length. The effect will be the more important the nearer to each other the anchor groups of the strings are, and it is expected to decrease as they are placed further apart. If string interference is the correct explanation for the observed lowering of inhibition efficiency, it allows us to test our estimates of string length.

The basic idea is this. If two strings interfere, it may be thought that their spheres of gyration overlap. By making a series of difunctional inhibitors in which the anchor groups are systematically placed further and further apart, it should be possible to find the distance at which interference ceases. At that point the inhibition factor of the difunctional inhibitor should be twice that of the monofunctional one, and the distance between anchors should be twice the radius of gyration of the string emanating from a single (unhindered) acceptor group.

We have chosen the naphthalene-1-sulfonic acid phenyl ester as the test acceptor,

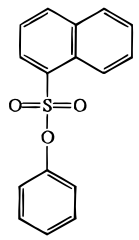

1

and we have made a series of difunctional inhibitors where the sulfonic acid groups are separated by structures that serve as distance pieces. These structures are indicated below. Q stands for the naphthalene sulfonic acid group.

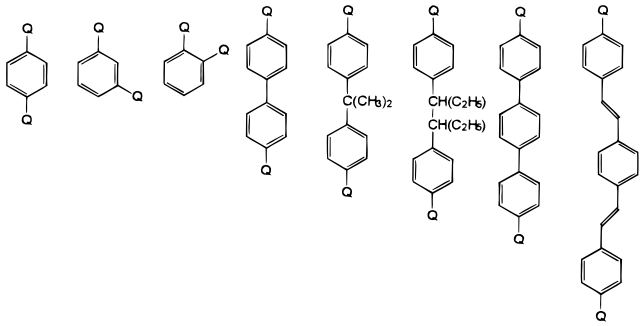

2a **2b** **2c** **3** **4** **5** **6** **7**

We measured the inhibition factors for the difunctional inhibitors (see Table 1). Since all the structures have the same acceptor group, the bracket in eq 3 will remain the same, and it is possible to determine the string length from the inhibition factor alone. In parallel to this we determined the geometric distance between anchors. We used a molecular modeling computer program[11] that is able to display a 3D representation of a molecule, find the configuration of minimum potential energy, and finally determine the distance between any two atoms of the molecule. These data are listed in Table 1.

In Figure 3 we have plotted (1/2)*f* for the molecules 2−7 as a function of the distance between their anchor groups (in angstrom units). We have used one-half the *f* number of the molecules as a measure of the inhibition strength of *a single anchor group* in the difunctional inhibitor to compare it with the inhibition strength of the string of a monofunctional naphthalene-1-sulfonic acid unit. The plot extrapolates to about 20 Å, which we believe to correspond to twice the radius of gyration of the monofunctional standard acceptor. The radius of gyration of the unhindred strings emanating from the sulfonic acid group is thus 10 Å.

Earlier we had calculated the radius of gyration of the strings of the sulfonic acid group directly from inhibition factors using eqs 3 and 4 and had found $R_G = \alpha \times 6.3$ Å.

For polymers of low molecular weight in good solvents the Flory−Fox factor[7] is of the order of $\alpha = 1.1$. This brings the expected value of the radius of gyration of the test acceptor to $R_G = 1.1 \times 6.3 = 6.9$, corresponding to a string length of $n = 12$. Compared with this, the radius of gyration found in the present experiments is clearly too large. The reasons for this discrepancy will be considered in the following when we discuss the relation between the overlap of the spheres of gyration of neighboring strings and the degree of their interference.

One would expect that the change in inhibition strength brought about by string interference would correlate with the overlap between the spheres of gyration of the interfering strings. That overlap corresponds to the spherical calottes indicated schematically in two dimensions in Figure 4. The volume of a calotte of height h in a sphere of radius R_0 is given by the formula

$$V(h) = (1/3)\pi h^2(3R_0 - h) \qquad (5)$$

For the strings of a difunctional inhibitor the overlap volume can be calculated from the radius of gyration

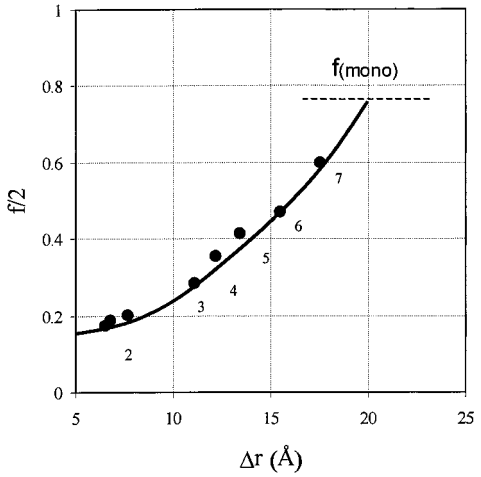

Figure 3. Plot of the inhibition factor of individual anchor groups, (1/2)*f*, against the spatial separation (Δ*r*) of the sulfonic acid anchor groups in a series of difunctional inhibitors.

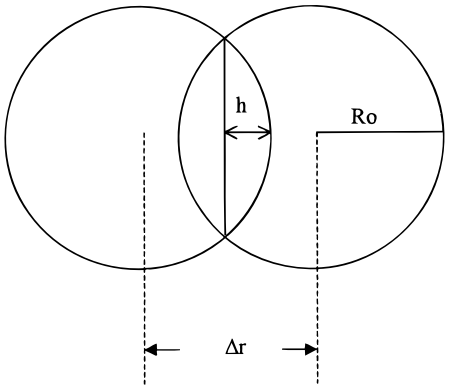

Figure 4. Characterizing the overlap of the spheres of gyration of strings emanating from the anchor group in a series of difunctional sulfonic acid inhibitors.

Table 1. Distance Δ*r* between Acceptor Sites and Inhibition Factor *f*

cmpd	Δ*r* (A)	*f*	cmpd	Δ*r* (A)	*f*
1 (mono)	(20)	0.77	**4**	12.2	0.712
2a	7.7	0.404	**5**	13.4	0.828
2b	6.8	0.374	**6**	15.5	0.94
2c	6.5	0.348	**7**	17.5	1.20
3	11.1	0.570			

$R_G = R_0$ of the test acceptor and the geometric separation (Δ*r*) of the anchor groups.

$$V(h) = (1/3)\pi(R_0 - 0.5\Delta r)^2(2R_0 + 0.5\Delta r) \qquad (6)$$

The fractional overlap volume $V(h)/V(R_0)$ is the ratio of the overlap volume to the volume of the whole sphere of gyration $V(R_0)$; the fraction of undisturbed volume of gyration is given by eq 7.

$$1 - \frac{V(h)}{V(R_0)} \qquad (7)$$

In Table 2 we have listed the fraction of the undisturbed volume of gyration for the individual difunctional inhibitors together with the inhibition factors of the difunctional inhibitors divided by *twice* the inhibition factor of the monofunctional inhibitor, $f/2f_0$. In Figure 5 we have plotted these data against each other. The correlation between the two quantities is not at all linear, which indicates that the effect of string interfer-

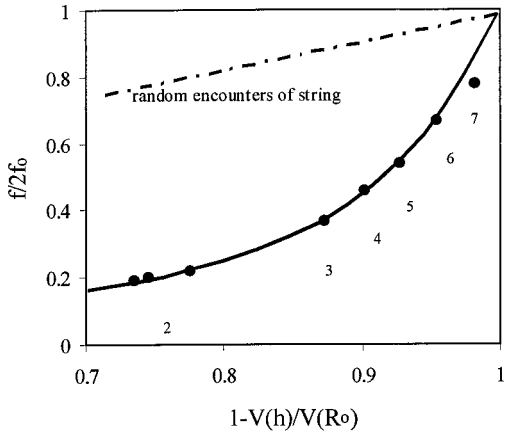

Figure 5. Relative inhibition factors of the anchor groups in a series of difunctional sulfonic acid inhibitors plotted against the fraction of undisturbed gyration volume or the strings.

Table 2. Geometric Separation, Fractional Overlap Volume, and Relative Inhibition Factor for a Group of Difunctional Naphthalene-1-sulfonic Acid Inhibitors

cmpd no.	Δr	$1 - V(h)/V(R_0)$	$f/2f_0$
1	20 A	1.0	1.0
2a	7.7	0.775	0.22
2b	6.8	0.745	0.20
2c	6.5	0.735	0.19
3	11.1	0.873	0.37
4	12.2	0.901	0.46
5	13.4	0.927	0.54
6	15.5	0.954	0.61
7	17.5	0.982	0.78

ence on the strength of inhibition is much larger than expected with regard to the overlap of the spheres of gyration. We conclude that the strings interfere more strongly than predicted simply for random encounters. There has to be an active element in the interference mechanism.

How can two strings interact? They cannot interact by hydrogen bonding because both are polarized in the same direction. Both offer a negatively polarized oxygen atom to the outside, and for that reason they cannot merge. However, the polarized OH groups of the ends of two *still growing* strings, and only those end groups, can interact with each other as electric dipoles. When the terminal members of two growing strings meet, they line up head-to-tail and form a quadrupolar configuration.

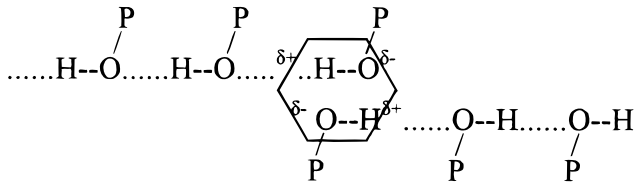

Within the quadrupolar complex the partial charges on the OH groups are compensated internally. They do not any more project an external field strong enough to hold another OH group: at the quadrupolar node the growth of both strings terminates.

It should be noted at this point that even quite weak interactions between two units are sufficient to profoundly change their encounter statistics. Conventional encounter statistics are derived with the assumption that at all times all points within the sphere of gyration have the same probability of carrying a phenolic unit. However, if two units stick together even for a limited time period, the probability that they will be together at a later moment (the moment of film deposition) is very much larger than predicted by random statistics. Hence the behavior demonstrated in Figure 5.

The results of this investigation can be summarized as follows: Phenolic strings emanating from nearby acceptor (anchor) groups interfere with each other. That is the rationale of the lowering of the inhibition factors of the individual strings in the multifunctional inhibitors of the semiconductor industry. It appears that the mechanism of interference is based on dipole−dipole interaction between the growing ends of the chains. The interference phenomenon was used to determine the natural radius of gyration (about 10 Å) of the generic naphthalene-1-sulfonic acid inhibitor.

Experimental Part

Materials. All the mesogenic biphenols were purchased from Aldrich Chemical Co. except compounds **6** and **7** and were used without further purification. The mesogenic biphenol **7** was a gift from Daniel J. Sandman (Lowell).

The general synthetic procedure used in making the difunctional inhibitors is described by the scheme below.

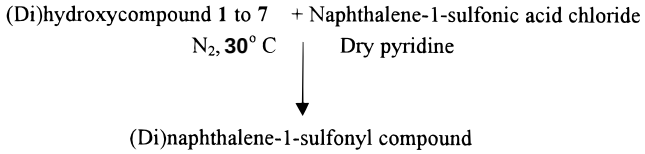

The mesogenic biphenols (0.01 mol) were dissolved in 50 mL of dry pyridine and then was added 0.022 mol of naphthalene-1-sulfonyl chloride, stirring under nitrogen for 16 h. The solutions were added dropwise into a 0.05 N HCl solution at 0 °C. The precipitate formed was filtered off and washed with a 0.05 N solution of sodium hydroxide. The product was finally crystallized from acetone/methanol (50/50) or chloform/methanol (50/50).

To prepare compound **6,** we had to make 4,4′-dimethoxy-*p*-terphenyl and 4,4′-di-hydroxy-*p*-terphenyl (see scheme below)

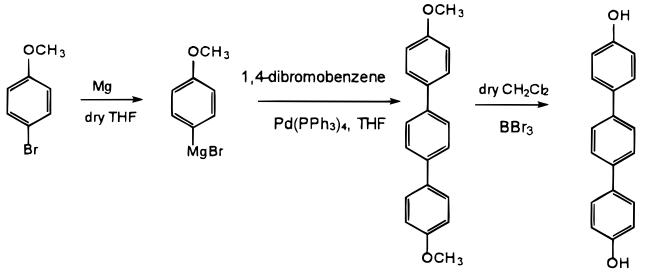

4,4′-Dimethoxy-p-terphenyl:[12] 4-Bromoanisole (0.1 mol, 11 mL) was added dropwise under nitrogen into dry THF (200 mL) containing magnesium turnings (0.12 mol) and dibromoethane (1 mL). Within 5 min the color of the solution changed to dark green. The remainder of the 4-bromoanisole was then added to the solution at a rate that allowed to maintain a moderate reflux. After 3 h, the 1,4-dibromobenzene (0.04 mol) was added dropwise to the solution. After that, $Pd(PPh_3)_4$ (0.3 mmol) was added to the still warm flask along with 10 mL of dry THF. The mixture was refluxed (85−95 °C) for another 8 h. After cooling, the solution was added to a 0.05 N aqueous HCl solution, filtered, and washed with water and acetone. The precipitated powder was added to a 10% NaOH solution, acidified, and filtered three times. The white platelets formed were recrystallized from benzene, yielding 2.5 g (45%); mp = 271 °C (lit. 273−275 °C).[13]

4,4′-Dihydroxy-p-terphenyl:[12] 4,4′-Dimethoxy-*p*-terphenyl (2.9 g, 0.01 mol) was added to dry CH_2Cl_2 (20 mL) at 0 °C, and the

BBr_3 was added slowly through a syringe. The reaction was stirred for 2 h at room temperature and then poured into ice water (200 mL). The precipitate that had formed was filtered and recrystallized from ethyl alchohol three times, yielding 1.89 g (75%); mp = 371 °C (DSC) with decomposition (lit. 375 °C).[13]

NMR Results and Melting Points. Compound **1**: ^{1}H NMR (acetone-d_6, 200 MHz), δ 6.9−7.25 (m, 5H, Ar−), 7.6−8.8 (m, 7 H, naphthalene); mp = 74−75.5 °C (DSC). Compound **2a**: ^{1}H NMR ($CDCl_3$, 200 MHz), δ 6.7 (s, 4H, Ar), 7.4−8.8 (m, 14 H, naphthalene); mp = 205−210 °C (DSC). Compound **2b**: ^{1}H NMR ($CDCl_3$, 200 MHz) δ 7.0 (dd, 2H, Ar), 7.15 (dd, 2H, Ar), 7.4−8.5 (m, 14 H, naphthalene); mp = 176−178 °C (DSC). Compound **2c**: ^{1}H NMR ($CDCl_3$, 200 MHz) δ 6.6 (t, 1H, Ar), 6.9 (dd, 2H, Ar), 7.3 (t, 1H, Ar) 7.7−8.5 (m, 14 H, naphthalene); mp = 143−147 °C (DSC). Compound **3**: ^{1}H NMR (acetone-d_6, 200 MHz) δ 6.9 (m, 4H, Ar), 7.4 (m, 4H, Ar), 7.4−8.8 (m, 14 H, naphthalene); mp = 173−175 °C (DSC). Compound **4**: ^{1}H NMR ($CDCl_3$, 200 MHz) δ 2.2 (s, 6H, $2CH_3$), 6.8 (d, 4H, Ar), 7.1 (d, 4H, Ar) 7.6−8.8 (m, 14 H, naphthalene); mp = 141−145 °C (DSC). Compound **5**: ^{1}H NMR (acetone-d_6, 200 MHz) δ 0.4 (m, 6H, $2CH_2CH_3$), 1.2 (m, 4H, $2CH_2CH_3$), 2.4 (m, 2H, 2CH−), 6.8 (m, 8H, −Ar−), 7.6−8.8 (m, 14 H, naphthalene); mp = 210−214 °C (DSC). Compound **6**: ^{1}H NMR (pyridine, 200 MHz) δ 6.5 (s, 4H, central−Ar−), 6.8 (dd, 8H, 2Ar), 7.6−8.8 (m, 14 H, naphthalene); degradation temperature = 345 °C (TGA). Compound **7**: ^{1}H NMR (pyridine, 200 MHz) δ 7.0−7.2 (dd, 4H, olefinic), 7.4 (dd, 8H, −Ar−), 7.5 (s, 4H, −central Ar), 7.6−8.8 (m, 14 H, naphthalene); degradation temperature = 341 °C (TGA).

Geometric Separation of Anchor Groups. The separation of the anchor groups of the individual inhibitors was determined from 3D molecular models generated by the program Chem 3D, CambridgeSoft Corp. This program was able to calculate the distance between the various anchor groups; we used an average value for the subsequent calculations. These are listed in Tables 1 and 2.

Dissolution Rate Measurements. Films were cast with a spin coater from Novolak solutions (25 wt % solids) containing the indicated quantities of inhibitor onto silicon wafers. The coatings were dried at 90 °C for 1 h. Their dissolution rate in 0.20 M KOH was measured at 20 °C with a laser interferometer described earlier.[14] The direct results of the dissolution rate measurements are shown in Figure 2.

Acknowledgment. We thank the Semiconductor Research Corporation for financial support of this work, and we are grateful to Daniel J. Sandman for the gift of the spacer compund **7**. We have benefited from discussions with Charles Szmanda of the Shipley Company and with Bruce Garetz and Peter Riseborough of Polytecnic University.

References and Notes

(1) Reiser, A.; Shih, H. Y.; Yeh, T. F.; Huang, J. P. *Angew. Chem., Int. Ed. Engl.* **1996**, *35*, 2428.
(2) Shih, H. Y.; Reiser, A. *Macromolecules* **1995**, *28*, 5595.
(3) Kim, M. S.; Reiser, A. *Macromolecules* **1997**, *30*, 4652.
(4) Yan, Zh.; Reiser, A. *Macromolecules* **1998**, *31*, 7723.
(5) Reiser, A. *Photoreactive Polymers*; Wiley: New York, 1989.
(6) Dammel, R. R. *Diazonaphthoquinone-based Resists*; SPIE Press: Bellingham, WA, 1993; Tutorial Text No. 11.
(7) Tanford, C. *Physical Chemistry of Macromolecules*; Wiley: New York, 1961; Chapter 3.
(8) Flory, P. J.; Fox, T. J. *J. Am. Chem. Soc.* **1951**, *73*, 1904.
(9) Szmanda, C. R.; Zampini, A.; Madoux, D. C.; McCants, C. L. *Proc. SPIE* **1989**, *1086*, 363.
(10) Uenishi, K.; Kawabe, Y.; Kokubo, T.; Slater, S.; Blakeney, A. *Proc. SPIE* **1991**, *1466*, 102.
(11) Chem 3D, version 4.0; Molecular Modeling and Analysis, CambridgeSoft Corp., Massachusetts, 1995.
(12) Nye, S. A.; Swint, S. A. *J. Polym. Sci. Part A: Polym. Chem.* **1994**, *32*, 721.
(13) Price, Ch. C.; Mueller, G. P. *J. Am. Chem. Soc.* **1944**, *66*, 632.
(14) Yeh, T. F.; Shih, H. Y.; Reiser, A. *Macromolecules* **1992**, *25*, 5345.

MA981090J